

Finite Element Modeling of Shear Failure in Prestressed Concrete AASHTO Girders

Alaa I. Chehab, PhD, Dept. of Civil & Env. Engineering, Wayne State University, Detroit, MI

Thai Dam, PhD, Dept. of Civil & Env. Engineering, University of Michigan, Ann Arbor, MI

Christopher D. Eamon, PhD, PE, Dept. of Civil & Env. Engineering, Wayne State University, Detroit, MI

Gustavo Parra-Montesinos, PhD, Dept. of Civil & Env. Engineering, University of Wisconsin, Madison, WI

ABSTRACT

Many studies concerning the shear behavior of prestressed concrete (PC) girders through experimental testing are available in the technical literature. However, few studies are specifically focused on the numerical modeling of prestressed concrete girder shear behavior. This study involved laboratory testing of two full-scale precast AASHTO Type II girder specimens. The purpose of the testing was to develop and validate numerical (finite element analysis; FEA) models that can accurately predict the shear capacity of precast pre-stressed concrete girders based on reliable experimental parameters, and to compare experimental results with ACI and AASHTO LRFD code calculated strengths in order to better understand the shear failure behavior in PC girders. Each girder was tested three times in different regions of the span by adjusting support locations to generate data for different critical shear span-to-depth ratios and stirrup spacing. Girders had stirrup spacing from 8 to 21 in. (203 to 533 mm) and shear span/depth ratios from 2.0 to 3.5. The developed FEA models were found to be reliable in predicting the shear capacity of PC girders, while design codes were found to lead to conservative calculated strengths.

Keywords: Pre-stressed concrete girder, Shear strength, Finite element analysis, AASHTO bridge girder

INTRODUCTION

Shear behavior in prestressed concrete (PC) girders was investigated in several studies through experimental testing, and was found to have inconsistency with the design codes calculated strengths. Ross et al. (2011) evaluated the structural condition of four AASHTO type III PC girders salvaged from a bridge in Florida. Girders were tested using a three-point loading scheme with five different a/d (shear span-to-depth) ratios ranging from 1.2 to 5.4. Laskar et al. (2010) present a simple shear design equation that was experimentally developed, based on tests of five full scale PC girders considering three primary variables: shear span-depth ratio (a/d), transverse steel ratio (ρ_t), and the presence of harped strands in the web. Saqan and Frosch (2009) investigated the shear strength and behavior of PC rectangular girders with prestressing strands and reinforcing bars, but without transverse reinforcement. Kuchma and Hawkins (2008) assembled a large experimental database, and evaluated the accuracy of different design methods based on the available test results. A total of 1359 girders were considered, from which 878 were reinforced concrete (RC) girders and 481 were PC girders. The majority of the PC girders were T-shaped and I-shaped, and had depths less than 20 in. Pei et al. (2008) conducted analytical and experimental studies of shear capacities of PC girders for bridges in Oklahoma. The study focused on AASHTO Type II girders designed according to the AASHTO Standard Specifications prior to the 1979 Interim provisions. De Silva et al. (2007) experimentally explored the shear cracking behavior of PC and RC girders. Tests were conducted on three I-shaped RC girders and four I-shaped PC girders. Hegger et al. (2004) used laser-interferometry and photogrammetry devices to attempt to gain insight to the shear resistance mechanism of PC girders by studying pre- and post-cracking behavior. Hartmann et al. (1988) evaluated the adequacy of AASHTO code provisions for shear capacity when applied to high strength PC girders with compressive strength from 10,800-13,160 psi. Similarly, Cumming et al. (1998) performed four shear tests on high-strength concrete prestressed girders.

Despite this large body of research, many fewer studies are specifically focused on the numerical modeling of prestressed concrete girder shear behavior. Some of this work includes that of Wilder et al. (2015), who conducted a parametric nonlinear finite element analysis to investigate the mechanical behavior of 9 full-scale PC I-shaped girders subjected to four-point loading. Mahesh and Surinder (2011) predicted the shear strength of RC and PC deep girders by using support vector regression (SVR). Here, a back-propagation neural network and empirical relations were used to model reinforced and prestressed concrete deep girders. Parametric studies with SVR suggested that concrete strength and the ratio of shear span to effective depth were particularly critical when predicting the strength of deep girders. Liu et al. (2011) discussed a method that uses inner transverse prestressing bars to enhance the shear capacity of concrete girders. Here, four transversely prestressed concrete girders and one ordinary reinforced concrete girder were modeled using a nonlinear finite element method. Laskar et al. (2010) discussed the development of the Cyclic Softened Membrane Model (CSMM), which has been efficiently used to predict the behavior of RC and PC girders critical in shear.

Design codes have utilized different methods for calculating the shear capacity of PC girders (AASHTO 2014, AASHTO 1983; ACI 318; Eurocode 2). In this study, the shear capacity expressions of two design codes are considered for comparison to the experimental and analytical results: those of the AASHTO LRFD Bridge Design Specifications (AASHTO 2014)

and ACI 318-14 (ACI 318, 2014). According to the AASHTO LRFD design procedure, the nominal shear resistance, V_n , (kips) of PC girders is taken as:

(1)

where in ksi.

Similarly, ACI 318-14 divides the nominal shear strength into contributions from concrete and steel transverse reinforcement. The nominal shear resistance, V_n (kips), may be computed using the following equations:

(2)

(3)

(4)

where in psi.

(5)

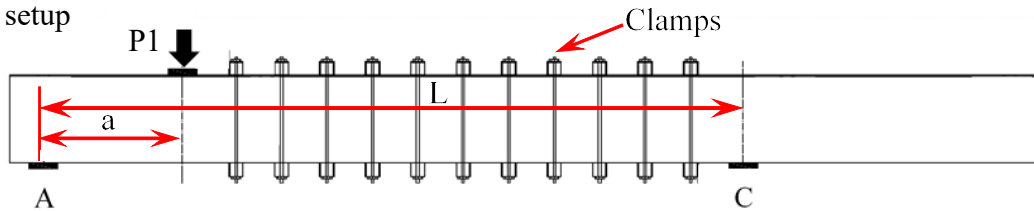
Here, V_c is the concrete shear capacity when cracking results from combined shear and moment, and V_{cw} is the web cracking shear capacity; V_s is the shear capacity of steel web reinforcement; V_p is the vertical component of pre-stressing force; λ is a factor indicating the ability of diagonally cracked concrete to transmit tension and shear; f'_c is the compressive strength in concrete; b_w is the effective web width; d is the effective shear depth, taken as the distance between the resultants of the tensile and compressive forces due to flexure; d_p is the distance from the extreme compression fiber to the centroid of prestressing steel; s is the spacing of transverse reinforcement; A_v is the area of shear reinforcement within a distance s ; f_y is the yield stress of the transverse reinforcement; α is the angle of inclination of diagonal compressive stresses; $\lambda = 1$ for normal weight concrete; V_d is the unfactored shear due to dead load; V_u is the factored shear load; M_{cr} is the moment causing flexural cracking; M_u is the factored moment; σ_c is the compressive stress in the concrete at the centroid of the section; and b_w is the width of the web.

As evidenced by the variety of competing methods available to predict the shear capacity of PC girders, no individual procedure is widely recognized to provide uniformly accurate results. Consequently, the development of a reliable procedure is highly desirable. Thus, the main objectives of this study were to: 1) develop and validate a finite element analysis (FEA) model that can accurately predict the shear capacity of PC bridge girders and; 2) to compare experimental and numerical results with ACI and AASHTO LRFD code calculated strengths.

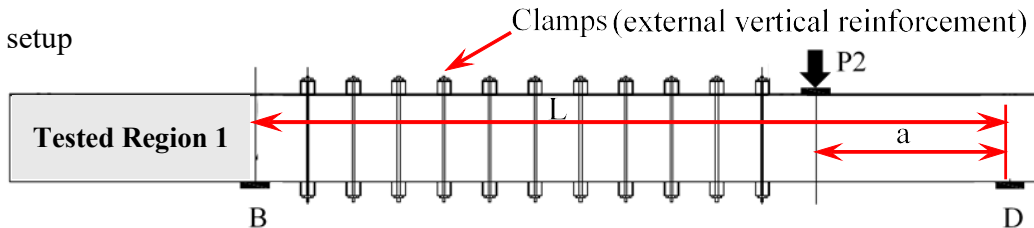
EXPERIMENTAL PROCEDURE

Two 36 ft long, full-scale PC AASHTO Type II girders were tested under various load configurations. Each girder was tested three times in different regions by adjusting support and load location (Tests 1, 2, and 3 shown in Fig. 1 (a) to Fig. 1(c)), to generate data for the a/d (span-to-depth) ratios and stirrup spacings of interest in this study. The load (P1, P2, P3) and support (A, B, C, D) positions for the three tests are shown in Fig. 1 (a) to (c). The girder test layout and cross section are also shown in Fig. 1.

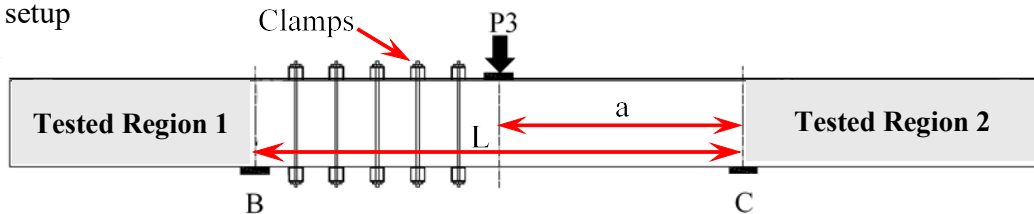
a) Test 1 setup



b) Test 2 setup



c) Test 3 setup



d) Reinforcement details

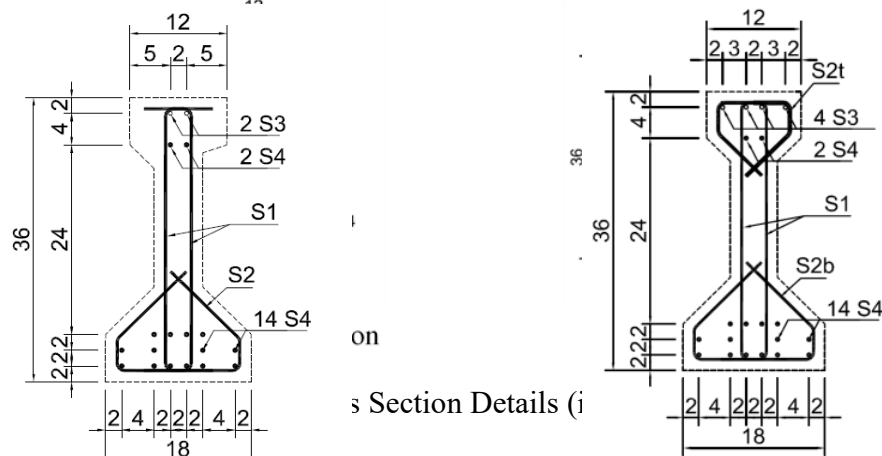


Fig. 1

Girder 1 Cross Section

Girder 2 Cross Section

Fig. 1 Girder Test Layout and Cross Section Details (inches)

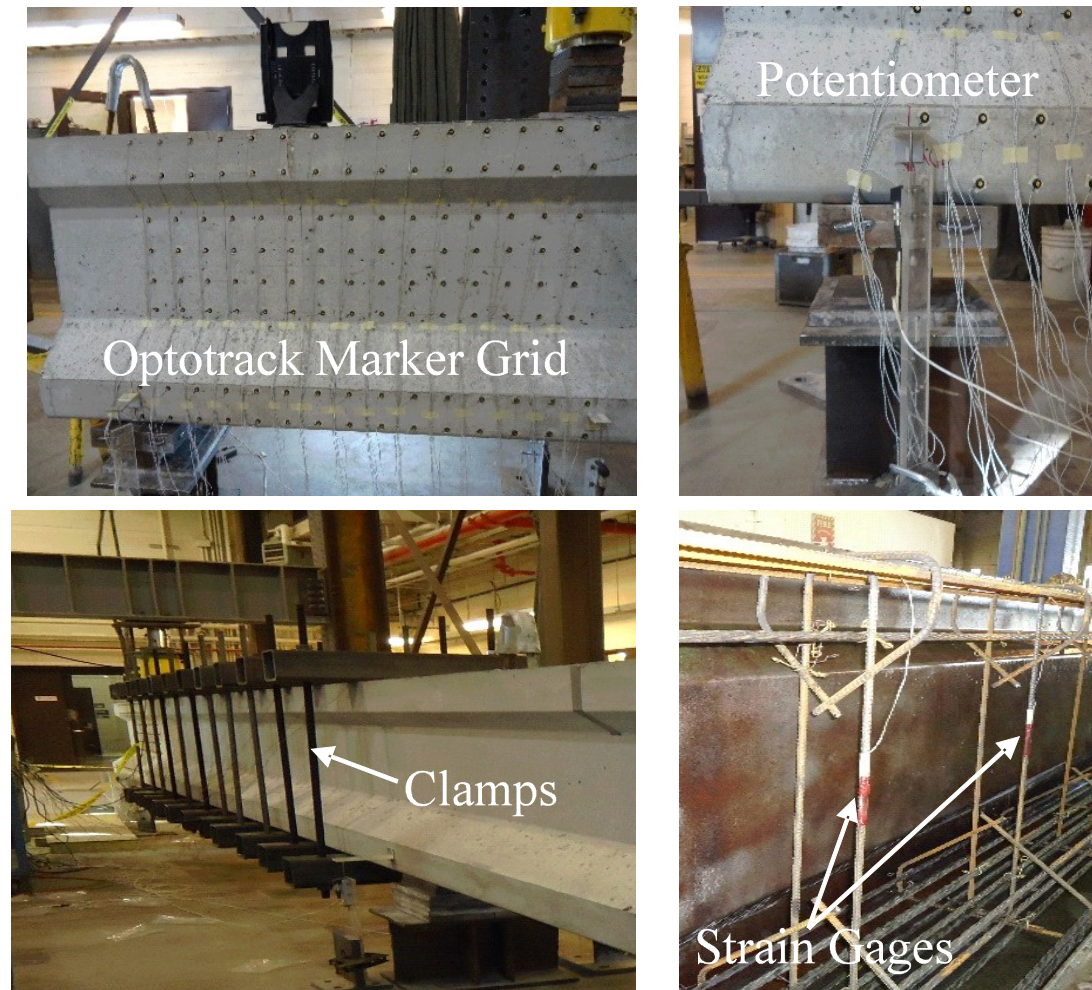


Fig. 2 Girder Test Instrumentation

For each girder, the portion of the span which was to be preserved for subsequent testing was externally clamped with vertical steel bars to prevent shear damage in this region during the prior tests. The girders were instrumented with strain gauges on transverse steel stirrups, an OptoTrack marker grid for measuring displacements on the girder exterior in the critical shear region, as well as potentiometers at supports and near the load location at the bottom of the girder, as shown in Fig. 2.

Reinforcement for two girders is shown in Fig. 1 (d). Pre-stressed steel reinforcement consisted of sixteen 1/2 in. seven-wire Grade 270 low-relaxation strands with a total area of 2.45 (labeled as S4) and an ultimate strength of 270 ksi. Each strand was prestressed with an initial force of 32 kips for Girder 1 and 26.5 kips for Girder 2. Mild steel reinforcement consisted of two and four #4 Grade 60 ($F_y = 60$ ksi) bars (labeled as S3) with a total area of 0.4 and of 0.8 at the top flanges of Girder 1 and Girder 2, respectively. Transverse reinforcement consisted of #3 Grade 60 double leg stirrups with an area of 0.22 (labeled as S1 and S2). Concrete had an average

cylinder compressive strength of approximately 8 ksi for Girder 1 and 9.2 ksi for Girder 2 at the testing days, with a coarse aggregate maximum-size of 0.75 in. and a total gross cross sectional area of 369 in². Stirrups spacing, a/d ratios, concrete cylinder compressive strength, and span dimensions for each girder test are shown in Table 1.

Table 1. Summary of Girder Parameters

	Tes					
	t	s (in)	f _c (ksi)	a/d	a (in)	L (in)
Girder 1	1	8.0	7.5	2.8	80	291
	2	8.0	7.8	3.4	98	309
	3	21.0	8.6	3.4	98	196
Girder 2	1	21.0	9.2	2.0	58	292
	2	21.0	9.2	2.8	81	315
	3	21.0	9.2	3.5	102	204

In each girder, a monotonic point load was applied using a hydraulic actuator resting on a 6 inch long steel plate centered at a distance of “a” from the support. Initially, load was applied at 20 kip increments until cracks were observed. After major cracks developed, the load was slowly increased until failure. Crack locations were recorded and tracked throughout the test with a marker to allow comparison to FEA results, as discussed below.

FINITE ELEMENT MODEL

Finite element modeling of the six girder tests was performed using Vector2 software (Wong et al., 2013). VecTor2 is based on the Modified Compression Field Theory (Vecchio and Collins, 1986) and the Disturbed Stress Field Model (Vecchio, 2000). It allows nonlinear analysis of two-dimensional reinforced concrete structures. Cracked concrete behavior is modeled in VecTor2 as an orthotropic material with smeared, rotating cracks. Girder models consisted of plane stress elements for concrete, and bar elements for longitudinal steel reinforcement, while transverse reinforcement was implicitly implemented with a smeared reinforcement model. Prestress force was applied as a pre-strain to the longitudinal reinforcing bar elements, which were considered to have full embedment with the concrete elements (i.e. no slip). These relatively simple models ranged in size from 4300-5500 elements, and the mesh was refined (minimum element size=1) at the section of interest where shear failure is was expected to occur, as shown in Fig. 3. For each test, only the girder length spanning between the location of the supports was modeled (as a simple span), as the additional span length of the girder beyond the supports has a negligible effect on the shear capacity at the critical section. Validation of the modeling approach was achieved by comparing numerical results to the test results.

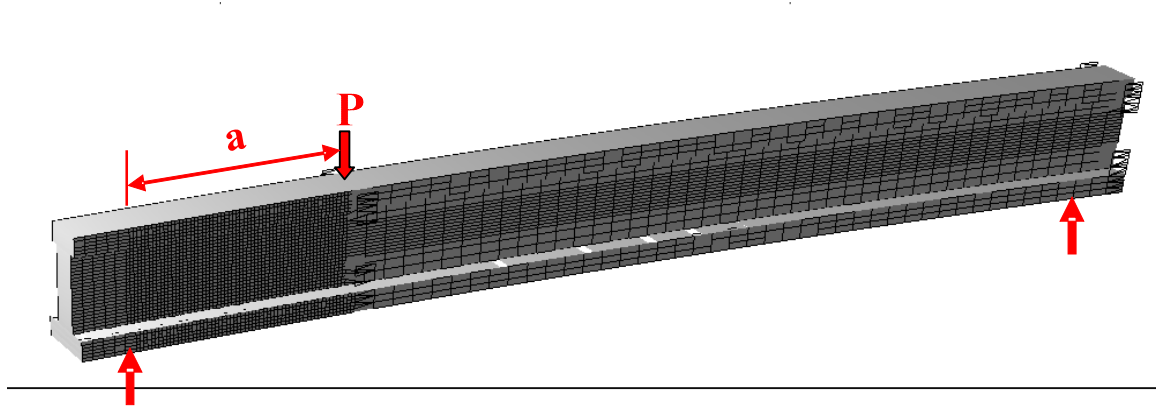


Fig. 3 Girder Finite Element Model (Girder1-Test 1).

RESULTS

The FEA model under-predicted test ultimate capacity by about 10% in all cases except for Girder 2-Test 2, which was under-predicted by about 30%, and in the case of Girder 2-Test 3, for which the predicted capacity matched the test result (within 1%). These results are summarized in Table 2, which also provides comparisons to the AASHTO LRFD and ACI code calculated nominal strengths. In contrast to the relatively close match of the FEA and test results, the LRFD method under-predicted test results by up to -240%, and by -148% on average. In general, the ACI procedure provided slightly more accurate results, under-predicting capacity by up to -150%, and by -96% on average, with less variation from test results, as shown by a lower coefficient of variation (COV) of experimental/code capacity ratios. Since the LRFD General Method was derived from the Modified Compression Field Theory (MCFT, Vecchio and Collins, 1986), contribution to shear from girder compression zone is neglected, and could be the main reason for such significant under-prediction in shear strength. Moreover, the effect of prestressing force was neglected, and could under-estimate the calculated shear strength.

Table 2. Summary of Test Results

	Test	Ultimate Shear Load/Capacity (kips)				Exp./FEA	Exp./LRFD	Exp./ACI
		Exp.	FEA	LRFD	ACI			
Girder	1	299	266	147	167	1.1	2.0	1.8
	2	262	239	148	168	1.1	1.8	1.6
	3	356	337	105	141	1.1	3.4	2.5
Girder	1	294	261	108	143	1.1	2.7	2.1
	2	271	214	108	143	1.3	2.5	1.9
	3	273	275	108	143	1.0	2.5	1.9
COV						0.09	0.23	0.17

Comparisons of the load-deflection curves of the experimental and FEA results are shown in Figs. 4 and 5.

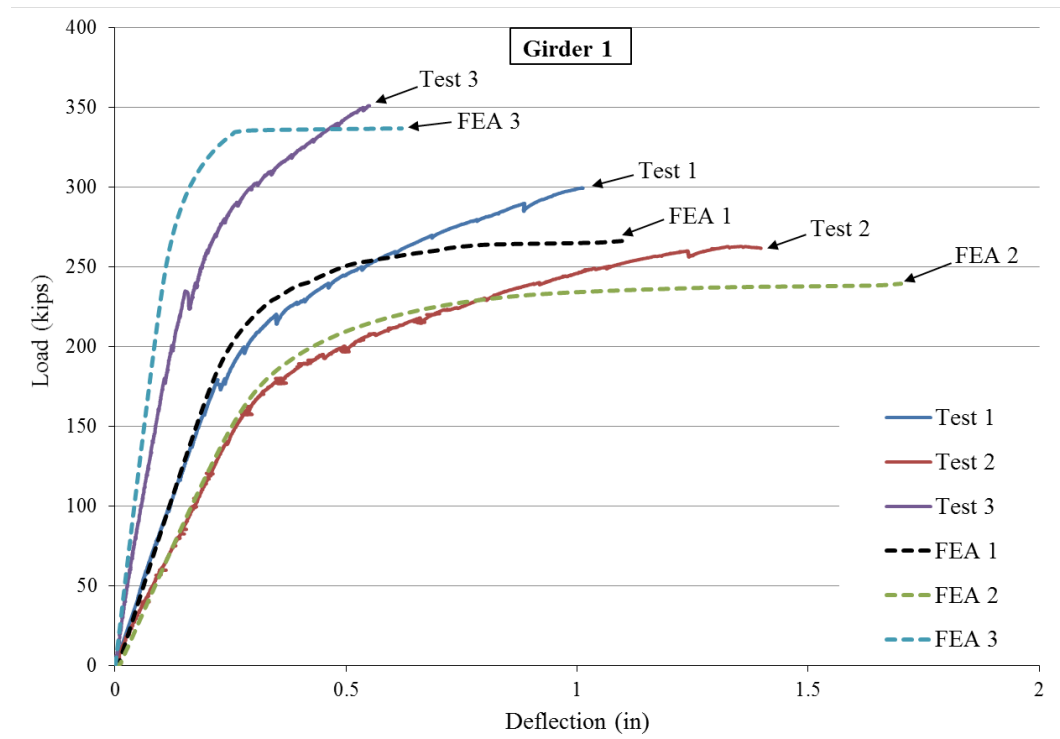


Fig. 4 Load versus Deflection Response (Girder 1)

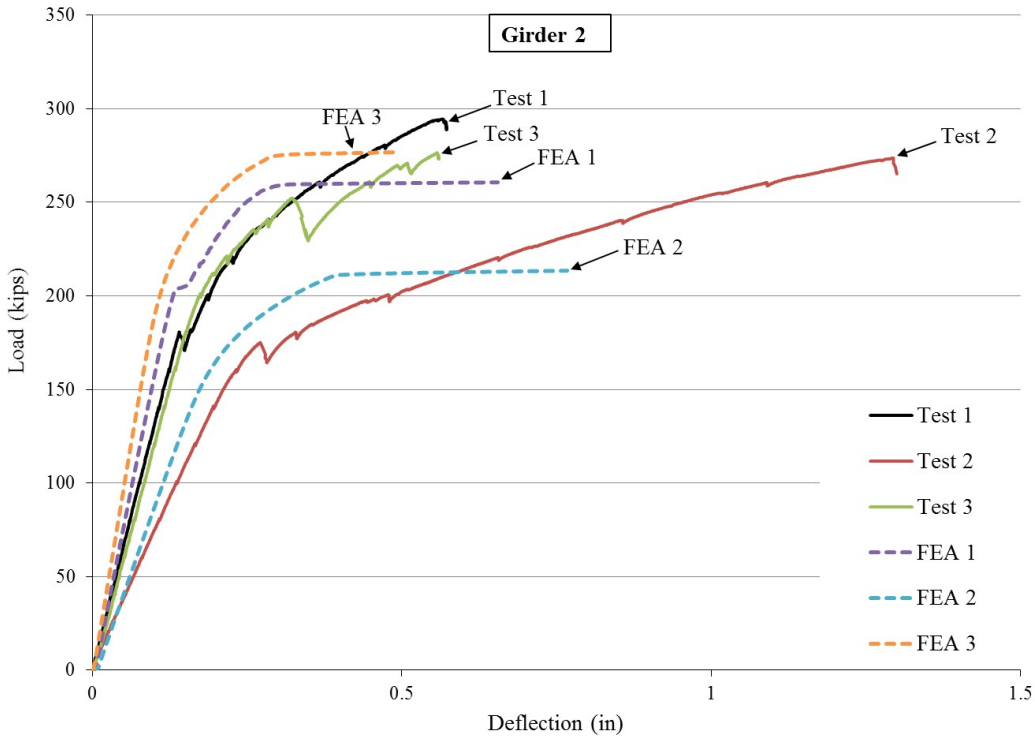


Fig. 5 Load versus Deflection Response (Girder 2)

As shown in the figures, the FEA model reasonably matched the load-deflection profile of the girders with only slight differences in initial stiffness (assumed to be prior to cracking). These initial differences may be due to support, load, and girder geometric idealizations, as well as possible minor and undetected cracks developed prior to testing. As shown, the most obvious discrepancies between test and FEA results are that tests display a stiffer post-yield behavior.

Comparisons between FEA and experimental results at failure are shown in Fig. 6. Here, the FEA model well predicted the failure mode and primary crack locations in the tested girders.

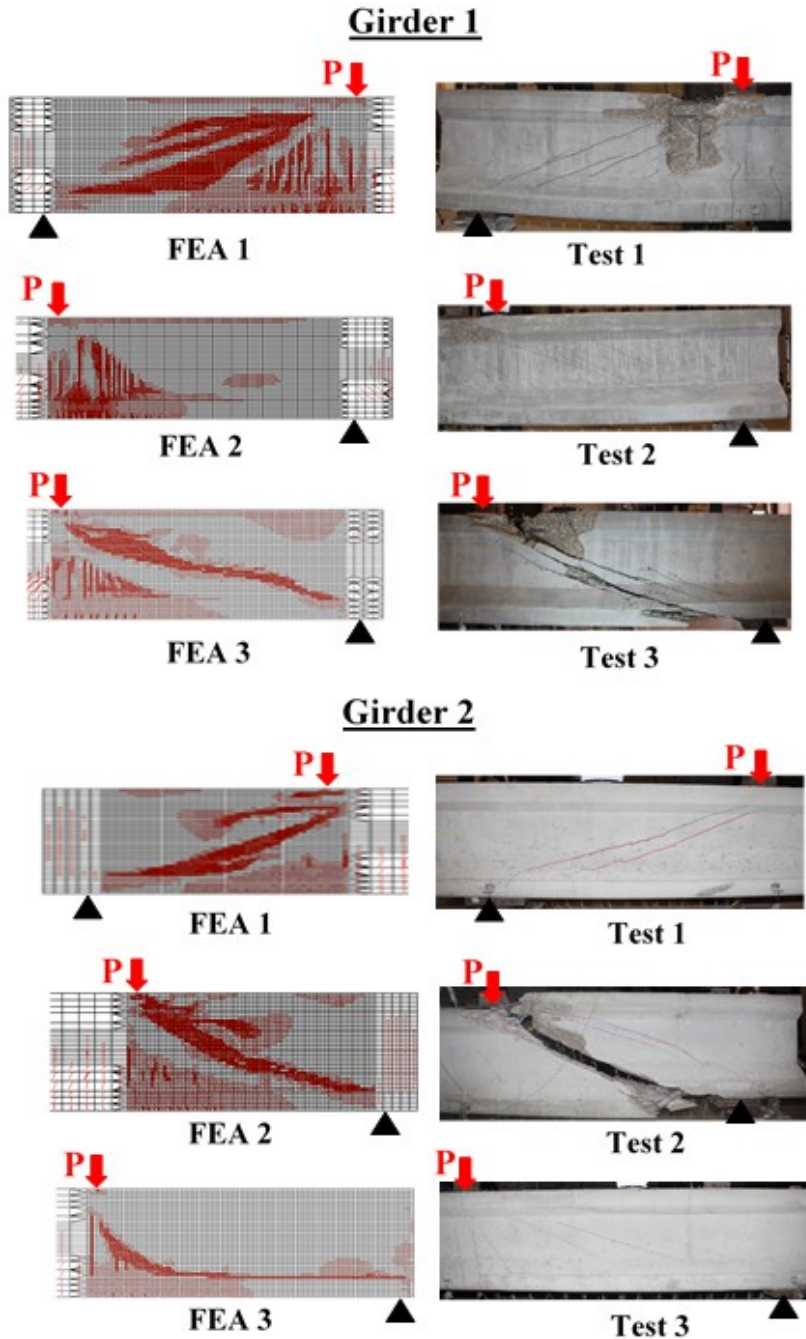


Fig. 6 FEA Model versus Test at Failure

To further investigate the contribution of the transverse steel in carrying shear forces, strain results from a typical case (Girder 1-Test 2) and the corresponding FEA model were compared. As shown in Fig. 7, steel yield strain was reached at gauges G13 and G14 prior to failure at approximately 262 kips in the test and at 239 kips in the FEA model. The FEA results show good agreement to the tests, and indicate that the transverse reinforcement did not carry significant load before approximately 200 kips of the applied load (for comparison, this test girder failed at 262 kips of applied load).

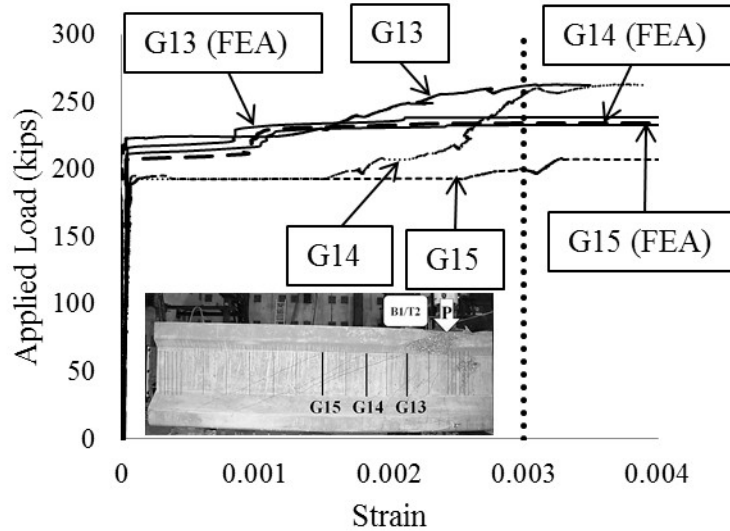


Fig. 7 Strain in Stirrups (Girder 1-Test 2)

SUMMARY AND CONCLUSIONS

Two 36 ft long, full-scale PC AASHTO Type II girders were tested in shear under monotonically increased concentrated loads. Each girder was tested three times in different regions by adjusting support and load location. Finite element analyses of the six girder tests were performed using a validated numerical model technique developed for this study. The shear capacity for each girder was computed using the AASHTO LRFD General Method and the ACI elaborate method, with the latter giving closer predictions to the actual tested shear capacities. However, code strength calculations were compared with experimental and numerical model results, and significantly underestimated the actual shear capacity of the tested girders. The FEA technique employed showed a relatively good agreement with the experimental results, and appears to be an accurate, slightly conservative approach to predict the shear capacity of PC girders. Given the large discrepancies between code approaches and the test results, further investigation of this subject is clearly needed.

ACKNOWLEDGEMENT

This research was supported by the Michigan DOT through grant # 2010-0298-Z5. The authors would like to thank Prof. James Wight, from the University of Michigan, for his help during the testing.

REFERENCES

1. AASHTO LRFD Bridge Design Specifications, 6th ed. American Association of State Highway and Transportation Officials, Washington, D.C., 2012.
2. AASHTO Standard Specifications for Highway Bridges, 12th ed. American Association of State Highway and Transportation Officials, Washington, D.C., 1983.

3. American Concrete Institute (ACI) Committee 318. 2014. Building Code Requirements for Structural Concrete (ACI 318-14) and Commentary (318R-14). Farmington Hills, MI: ACI.
4. CEN. Eurocode 2: Design of concrete structures - Part 1-1: General rules and rules for buildings, 2004.
5. Cumming, D. A., French, C. E., and Shield, C. K. "Shear Capacity of High-Strength Concrete Prestressed Girders". Minnesota Department of Transportation. p 396. May 1998.
6. De Silva, S., Mutsuyoshi, H., and Witchukreangkrai, E. "Evaluation of shear crack width in I-shaped prestressed reinforced concrete girders". Journal of Advanced Concrete Technology, v 6, n 3, p 443-458, October 2008.
7. De Wilder, Kristof, et al. "Stress field based truss model for shear-critical prestressed concrete girders." *Structures*. Vol. 3. Elsevier, 2015.
8. Hartmann, D. L., Breen, J. E., and Kreger, M. E. "Shear Capacity of High Strength Prestressed Concrete Girders", University of Texas at Austin, Center for Transportation Research. Report: CTR-3-5-84-381-2, 271 p, Jan 1988.
9. Hegger, J., Sherif, A., and Görtz, S. "Investigation of Pre- and Postcracking Shear Behavior of Prestressed Concrete Girders Using Innovative Measuring Techniques". ACI Structural Journal, v 101, n 2, p 183-192, March/April 2004.
10. Kuchma, D. A., Hawkins, N. M., et al. "Simplified Shear Provisions of the AASHTO LRFD Bridge Design Specifications". PCI Journal, v 53 n 3, p 53-73, May-June 2008.
11. Laskar, A., Hsu, T. C., Mo, Y.L. "Shear strengths of prestressed concrete girders part 1: Experiments and shear design equations". ACI Structural Journal, v 107, n 3, p 330-339, May-June 2010.
12. Laskar, A., Howser, R., Mo, Y.L., Hsu, T.T.C. "Modeling of prestressed concrete bridge girders". Proceedings of the 12th International Conference on Engineering, Science, Construction, and Operations in Challenging Environments - Earth and Space 2010, p 2870-2887, 2010.
13. Liu, Can, Bo Wu, and Kai Yan Xu. "Parametric Study on Reinforced Concrete Beams with Transversely Prestressed Bars." Applied Mechanics and Materials. Vol. 105. Trans Tech Publications, 2012.
14. Mahesh, P., Surinder, D. "Support vector regression based shear strength modeling of deep girders". Computers and Structures, v 89, p 1430-1439, April 2011.
15. Pei, J. S., Martin, R. D., Sandburg, C. J., and Kang, T. H. "Rating Precast Prestressed Concrete Bridges for Shear". FHWA-OK-08-08. December 2008.
16. Ross, b. E., Ansley, M., Hamilton, H. R. "Load testing of 30-year-old AASHTO Type III highway bridge girders". PCI Journal, p 152-163, 2011.
17. Saqan, E., Frosch, R. J. "Influence of flexural reinforcement on shear strength of prestressed concrete girders". ACI Structural Journal, v 106, n 1, p 60-68, Jan-Feb 2009. Transversely Prestressed Bars." Applied Mechanics and Materials, v 105-107, p 912-917, 2012.
18. Vecchio, F.J. and Collins, M.P. "The Modified Compression-Field Theory for Reinforced Concrete Elements Subjected to Shear." ACI Journal, March-April 1986.
19. Wong, P., Vecchio, F. J. and Trommels, H. (2013), "VecTor2 and FormWorks manual", 2nd edition, University of Toronto, Toronto, Canada.